Bull. Chem. Soc. Ethiop. **2024**, 38(1), 123-134.
DOI: https://dx.doi.org/10.4314/bcse.v38i1.10

ISSN 1011-3924
Printed in Ethiopia
Online ISSN 1726-801X

GREEN SYNTHESIS OF IRON OXIDE NANOPARTICLES FROM *SPERMACOCE OCYMOIDES BURM.F.* PLANT EXTRACTS FOR TARGETED LUNG CANCER A549 CELL THERAPY

T. Uma Rajalakshmi[1], C. Esaivani[2], T. Anantha Kumar[3], R. Mariselvam[4,5], G. Tamil Selvan[4], Zhen Zhang[4], Nouf M. Alyam[6] and P. Mariselvi[1*]

[1]Department of Chemistry, Rani Anna Government College for Women, Manonmaniam Sundaranar University, Tirunelveli, Tamil Nadu, India - 627602
[2]PG Department of Zoology, Sarah Tucker College (Autonomous), Tirunelveli, Affiliated to M.S. University, Tirunelveli, Tamil Nadu, India
[3]Department of Chemistry, Merit Arts and Science College, Idaikkal, Tirunelveli, Tamil Nadu, India - 627602
[4]School of the Environment and Safety Engineering, Jiangsu University, Zhenjiang - 212013, China
[5]Saraswathi Institute of Lifescience, Alangulam Main Road, Terkkumadathur - 627423, Tenkasi, Tamil Nadu, India
[6]Department of Zoology, College of Science, King Saud University, PO Box - 2455, Riyadh, 11451, Saudi Arabia

(Received September 14, 2023; Revised October 11, 2023; Accepted October 12, 2023)

ABSTRACT. The present study evaluated the synthesis of iron oxide nanoparticles using *Spermacoce ocymoides* Burm.f. plant extracts, and the effects of plant based iron oxide nanoparticles on A549 lung cancer cells were investigated to elucidate their impact on cellular morphology, mitochondrial function, and apoptotic pathways. *Spermacoce ocymoides* plant based iron oxide nanoparticles were characterised by X-ray diffraction, Atomic force microscopy, FTIR, and UV-Vis absorption spectroscopy. Iron oxide nanoparticle treatment caused considerable morphological alterations in A549 cells, including cell shrinkage, detachment, membrane blabbing, and distorted shape, consistent with cellular stress and potential apoptotic events. MMP analysis revealed a dose-dependent decrease in mitochondrial membrane potential, implying that nanoparticles have an effect on mitochondrial function. The presence of reactive oxygen species suggested that oxidative stress was involved in the cellular response to iron oxide nanoparticles. Additionally, DNA fragmentation analysis confirmed the activation of apoptotic pathways, with the nanoparticles themselves serving as a positive control for inducing apoptosis. The observed morphological changes, altered mitochondrial function, ROS production, and DNA fragmentation collectively point towards apoptotic cell death pathways being triggered by the nanoparticles.

KEY WORDS: *Spermacoce ocymoides*, Iron oxide nanoparticles, A549 cells, Apoptotic

INTRODUCTION

Lung cancer is one of the most common cancers in the world, both in terms of new cases diagnosed and fatalities caused (incidence and mortality) [1]. According to the World Health Organisation (WHO), lung cancer accounted for roughly 11.6% of all new cancer cases and 18.4% of all cancer-related deaths in 2020. It is the leading cause of cancer death in both men and women worldwide [2]. Lung cancer is a type of cancer that starts in the lungs. It occurs when normal lung cells have genetic alterations that let them to grow uncontrollably, culminating in the formation of a tumour. This tumour can compromise lung function and spread to other parts of the body through the circulation or lymphatic system, a process known as metastasis [3]. Non-small cell lung cancer (NSCLC) and small cell lung cancer (SCLC) are the two forms of lung cancer.

*Corresponding author. E-mail: mariselviveil@gmail.com

NSCLC is the most common kind, accounting for roughly 85% of all cases of lung cancer. SCLC is less prevalent, but it is more aggressive and spreads faster [4]. Tobacco use is the leading cause of lung cancer, including both active smoking and second hand smoke exposure [5]. Risk factors include exposure to environmental toxins (such as radon, asbestos, and certain chemicals), a family history of lung cancer, and a history of previous lung problems [6]. Lung cancer symptoms include a persistent cough, chest pain, shortness of breath, hoarseness, coughing up blood, weight loss, and fatigue. However, symptoms can vary depending on the stage and kind of lung cancer [7].

Lung cancer is a major global health issue that has a considerable influence on public health, affecting millions of individuals globally. The following are some significant characteristics of the worldwide perspective on lung cancer [8]. Regional variations in the incidence and mortality rates of lung cancer vary greatly around the globe. High-income countries have greater rates of lung cancer, owing to higher rates of tobacco smoking and other risk factors. However, lung cancer is becoming more of a problem in some low- and middle-income nations as tobacco smoking and environmental risk factors rise [9]. Lung cancer is a major public health issue in India, with an increasing incidence and mortality rate. It is one of the main causes of cancer-related mortality in the United States. The prevalence of lung cancer in India is influenced by a number of factors [10]. Tobacco use is the leading cause of lung cancer in India, as it is in many other areas of the world. Tobacco usage is widespread in India, and there are a considerable number of smokers. Tobacco smoking, including gutka, pan masala, and beedi, as well as air pollution from metropolitan areas, automotive emissions, industrial operations, and building sites, can all contribute to respiratory issues and lung cancer instances [11, 12].

The single most important risk factor for lung cancer is tobacco smoking. The majority of occurrences of lung cancer are directly related to smoking cigarettes, cigars, or pipes. Lung cancer rates vary across countries and regions, much as smoking rates do [13]. In addition to active smoking, second hand smoke exposure is a risk factor for lung cancer. This suggests that even nonsmokers who are exposed to tobacco smoke in their environment are more likely to get lung cancer [14]. Exposure to environmental pollutants (such as radon, asbestos, and certain chemicals), occupational exposure to carcinogens, a family history of lung cancer, and a history of lung diseases such as chronic obstructive pulmonary disease (COPD) are all risk factors for lung cancer, in addition to smoking [15].

Treatment options for lung cancer have evolved significantly in recent years. Personalized medicine, targeted therapies, immunotherapy, and other innovative treatments have shown promising results in some cases, improving survival rates and quality of life for certain patients [16, 17]. The cost of cancer treatment can vary greatly from country to country due to differences in healthcare systems, drug prices, and overall economic conditions. Overall, cancer treatment is expensive and has side effects [18]. So we need an alternative to treat the cancer. Recent research has focused on plants for treating cancer. Many plants and natural compounds have been studied for their potential to treat or support the treatment of cancer. However, it's important to note that while some of these compounds may have shown promising results in laboratory or animal studies, their effectiveness and safety for treating cancer in humans are still being researched [19]. Cancer treatment should always be discussed with qualified medical professionals, and natural remedies should not be used as a replacement for evidence-based medical treatments [20]. Here are a few examples of plants and compounds that have been studied for their potential cancer-fighting properties; *Taxus brevifolia* (taxol) [21], *Catharanthus roseus* (vinblastine and vincristine) [22], *Curcuma longa* (curcumin) [23], *Camellia sinensis* (catechins) [24], *Zingiber officinale* [25], *Allium sativum* [26] (organosulfur compounds), *Viscum album* [27] (mistletoe), *Panax quinquefolius* [28] (ginseng), *Aloe Vera* [29], *Echinacea purpurea* [30], etc.

Nanotechnology is the creation, manipulation and use of materials at the nanometer size scale (1 to 100 nm). There is a tremendous growth in the field of nano science and nanotechnology over the past two decades. Nanomaterials have numerous applications in the field of electronics,

cosmetics, coatings, packaging and biotechnology [31]. Metal oxide nanoparticles (NPs) are categorized as engineered nanomaterials that are widely known recently [32], and among them, iron oxide nanoparticles are extensively produced, within the world. Numerous metal oxides, including iron oxide, nickel oxide, zinc oxide, copper oxide, silver oxide, titanium dioxide, tin oxide, magnesium oxide, silicon, and gold oxides, have numerous uses in the environment (detection of toxins and pollutants, remediation, photo degradation, and water treatment), catalysis, the textile industry, electronics (batteries, optical limiting devices, and gas sensors), mechanical industries, and the pharmaceutical sector (cancer therapy, d-aspartame, and other drugs). One of the most biocompatible metal oxide nanoparticles is iron oxide, which has remarkable microscopic physical properties like superparamagnetism, firmness in liquid solution, low susceptibility to oxidation, long blood half-lives, and flexible surface chemistry. Iron oxide has a wide range of applications in environmental regulation, such as antibiotic degradation, adsorption of dyes, food-related processes, biomedical (drug delivery, magnetic cell sorting, magnetic resonance imaging (MRI) [33]. Nanoparticles have gained significant attention in the field of cancer treatment due to their unique properties and potential to improve the delivery and effectiveness of therapeutic agents [34]. These tiny particles, typically in the range of 1 to 100 nanometers, can be engineered to carry drugs, genes, or other therapeutic payloads directly to cancer cells [35]. So, the present deals with the green synthesis of Iron oxide nanoparticles using *Spermacoce ocymoides* plant extracts to treat lung cancer A549 cells.

EXPERIMENTAL

Plant collection and extraction

Fresh green leaves of *Spermacoce ocymoides* were collected from the Merit Arts and Science College campus in Idaikal at the GPS Coordinates range of Latitude at 8° 76’ 54.2224” N and Longitude 77° 45' 11.5067” E, Ambasamudram, Tamil Nadu, India during the period of December 2022. The leaves were collected, washed, and dried. The process was performed 2-3 times to remove all dust and undesirable particles. *Spermacoce ocymoides* leaves were cleaned and cut into fine bits before being added to 500 mL beakers containing 200 mL double distilled water. The combinations were boiled for one hour at 100 °C. The mixture was then cooled to room temperature. The extracted leaves were filtered through Whatman number 1 filter paper. The extracted materials were then used to create iron oxide nanoparticles.

Preparation of iron oxide nanoparticles

The 0.1 M $FeCl_2$ aqueous solution was generated using double distilled water and was then utilised to synthesise iron oxide nanoparticles. In a conical flask, leaf extracts of *Spermacoce ocymoides* were combined with a freshly made 0.1 M $FeCl_2$ solution and swirled constantly for 15 min. The solution of the mixture changes colour from yellow to dark brown. The mixture's hue altered, indicating the development of iron oxide nanoparticles. After draining the supernatant, the nanoparticles were collected [36]. The nanoparticles were collected and stored in dark glass bottles.

Characterization of iron oxide nanoparticles

Using advanced microscopic techniques such as X-ray diffraction (XRD), atomic force microscopy (AFM), FTIR, and UV-Vis absorption spectroscopy, nanoparticles are distinguished primarily by their size, shape, and surface charge. The average particle diameter, size distribution, and charge all have an impact on the physical stability and in vivo distribution of nanoparticles.

Anticancer studies of iron oxide nanoparticles against A549 cells

MTT assay Mosmann (1983) method was used to assess the cytotoxicity of *Spermacoce ocymoides* plant extracts based on iron oxide nanoparticles on A549 cells.

Cell culture. The AGS cell lines were obtained from India's National Centre for Cell Sciences (NCCS). For cell maintenance, 10% foetal bovine serum was added to Dulbecco's Modified Eagle Media. In addition to the media, antibiotics such as penicillin (100 U/mL) and streptomycin (100 µg/mL) were utilised. The cell lines were kept at 37 °C in optimal humid conditions with 5% CO_2.

Cell viability assay. The cytotoxicity assay of the selected nanomaterials on A549 cells was performed as by Riss *et al.* [37] with some modifications. The reduction of the MTT reagent was done by the viable cells through their mitochondrial dehydrogenase enzyme. Eventually, this process results in purple colour formation, which will be analysed further by dissolving it in an appropriate solution, and absorbance is measured at 540 nm by a plate reader. The MTT assay was performed for the untreated cancer cells and the green synthesised iron oxide nanoparticle-treated cancer cells as described above, with concentration ranges of 10 µL and 15 µL. Further IC_{50} values were calculated based on the MTT analysis.

AO/EB staining for the detection of cell death

A549 cells were seeded at 5 x 104 cells/well in a 6-well plate and cultured for 24 hours. After 24 hours of treatment with iron oxide nanoparticles (10 and 15 µg), the cells were separated, rinsed with cold PBS, and dyed for 5 min at room temperature with an AO (100 µg/mL)/EB (100 µg/mL) ratio (1:1). The stained cells were examined under a fluorescent microscope at a magnification of 20x. At the completion of the therapy, the cells were collected and washed three times with PBS. After 5 min of staining with acridine orange/ethidium bromide (AO/EB 1:1 ratio; 100 µg/mL), the plates were examined under a fluorescence microscope at 20x magnification. The overall count of apoptotic cells was calculated as a percentage of the total number of cells in the field.

Detection of ROS using carboxy-H2DCFDA

Carboxy-H2DCFDA is not luminous, however when oxidised in the presence of ROS, it becomes fluorescent green. Prepare a fresh stock solution of carboxy-H2DCFDA in sterile dimethyl sulfoxide (DMSO) or 100% ethanol immediately before use. After 24 hours of treatment with medicines at the IC_{50} concentration, employ carboxy-H2DCFDA in a normal culture medium with decreased serum (2%). Incubate the cultures for 30 minutes in a standard incubator in the dark (37 °C, 5% CO_2). All unused dye solutions should be discarded. Wash the carboxy-H2DCFDA-containing media twice with HBSS or PBS. From now on, the cells should be shielded from light. Incubate the carboxy-H2DCFDA-loaded cells in new media with your medication of choice. The cells were immediately visualised using a fluorescence microscope (Zoe Fluorescent Cell Imager, Biorad).

Mitochondrial membrane potential by Rhodamine 123 staining

Rhodamine 123 staining is a widely used technique to assess mitochondrial membrane potential ($\Delta\psi m$) in cells. Mitochondrial membrane potential refers to the electrical potential difference cross the inner mitochondrial membrane, which is generated by the proton gradient formed during electron transport in the process of oxidative phosphorylation.

RESULTS AND DISCUSSION

Fourier Transform Infrared Spectroscopy (FTIR) examination gives information about the chemical bonding and molecular structure of the iron oxide nanomaterial that was synthesised (Figure 1). FTIR measurements in the 400-4000 cm^{-1} range are performed at room temperature to analyse the composition and crystalline quality of the synthesised -Fe_2O_3 nanoparticles. The image showed absorption bands at 3451, 2979, 1498, 1043, 926, 842, and 468 cm^{-1}. The band at 3451 and 2979 cm^{-1} corresponds to the stretching of the OH bond and represents the aqueous phase, with a rise in the absorption band showing ferric chloride reduction. The 1498 cm^{-1} peak corresponded to C-H bending vibration. The presence of C-H stretching vibrations is shown by the band at 1043 cm^{-1}. The establishment of the Fe-O bond is responsible for the creation of the strong absorption bands at 617 and 468 cm^{-1}, which clearly indicates the formation of iron oxide nanoparticles. Fe-O-H stretching vibration is connected with the band at 617 cm^{-1}.

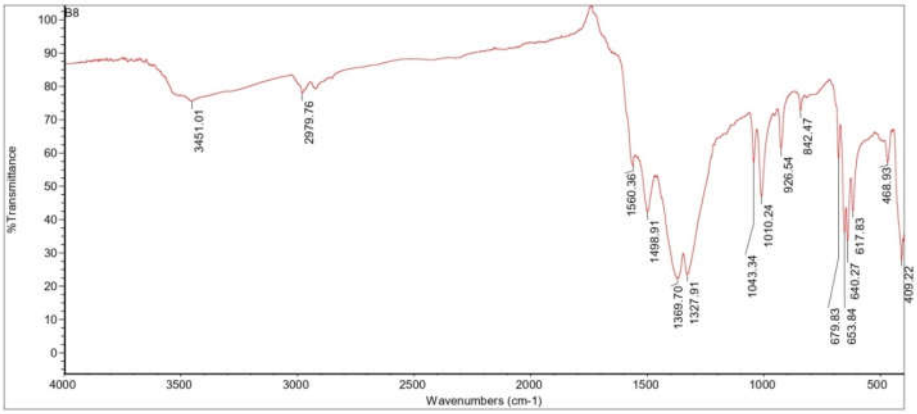

Figure 1. FTIR analysis of iron oxide nanoparticles using *Spermacoce ocymoides* plant extracts.

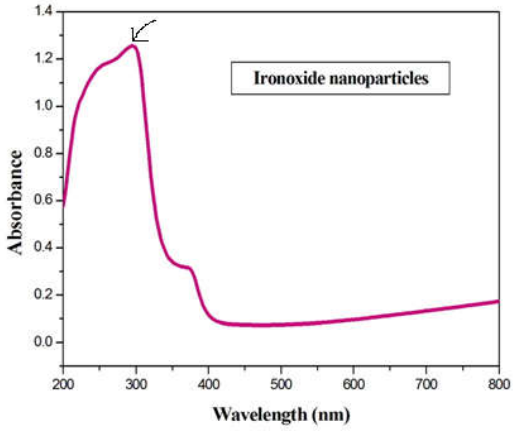

Figure 2. UV-Visible spectra of iron oxide nanoparticles using *Spermacoce ocymoides* Plant extracts.

Figure 2 depicts the UV-Vis absorption spectra of an iron oxide nanoparticle at ambient temperature. The presence of iron oxide nanoparticles is indicated by absorbance peaks at 290-300 nm.

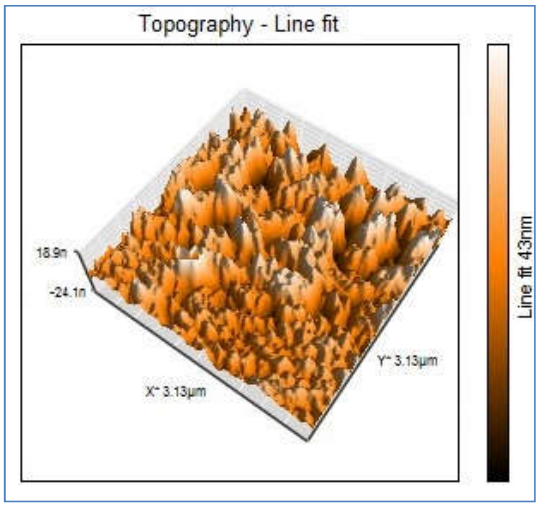

Figure 3. AFM image of iron oxide nanoparticles using *Spermacoce ocymoides* plant extracts.

The surface roughness of the sample was determined using atomic force microscopy (AFM). The surface roughness was found to be in the range of 1.67 µm to 1.75 µm. The surface structure of the synthesised iron oxide nanoparticles was investigated using an atomic force microscope (AFM), as illustrated in Figure 3. The discovered mountain-like structure of the iron oxide nanoparticle may be seen in the 3D image.

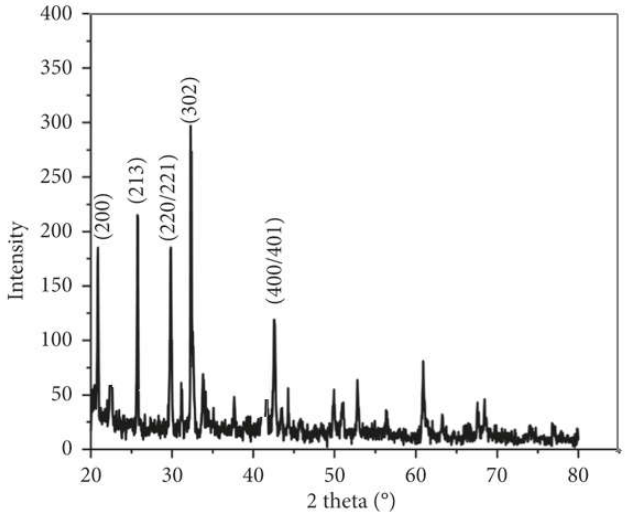

Figure 4. XRD spectra of iron oxide nanoparticles using *Spermacoce ocymoides* plant extracts.

The image depicts the X-ray diffraction spectrum of the synthesised nanoparticles. The iron oxide nanoparticles' X-ray diffraction was measured at two different values ranging from 10 to 80. The crystalline phase of iron oxide nanoparticles is represented by the indexed diffraction peaks depicted in Figure 4. The existence of iron oxide nanoparticles indicates that hematite-Fe_2O_3 nanocrystals have formed. The Debye Scherrer equation ($D = 0.9/\beta\cos\theta$) was used to get the average crystallite size D, where is the X-ray wavelength, is the Braggs angle in radians, and is the peak's total width at half maximum. The average crystallite size D was found to be 36.4 nm. Crystallite size becomes especially important when dealing with nanomaterials. Understanding and controlling crystallite size is crucial in the development of nanomaterials with unique properties for various applications, including medicine.

Khan *et al.* [38] recently noticed a combination of -Fe_2O_3 and -Fe_2O_3 in sol-gel produced iron oxide following a 600 °C heat treatment. Das *et al.* [39] used a hydrothermal reaction after thermal heating in a hydrogen/argon environment at 300 °C to transition from -Fe_2O_3 to Fe_3O_4 phases.

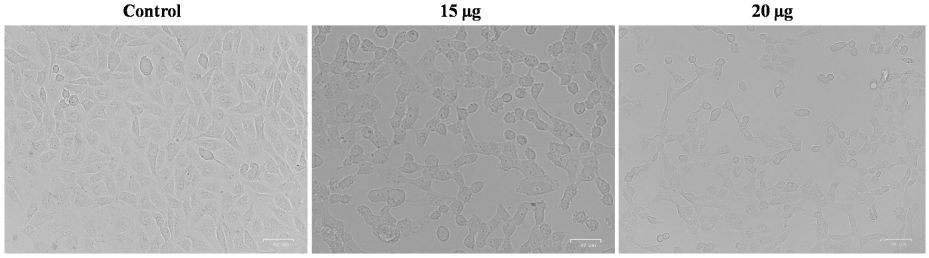

Figure 5. Morphological changes in control and sample 20 treated Lung Cancer A549 cells for 24 h.

Iron oxide nanoparticle treatment (15 and 20 µg/mL for 24 h) produced morphological alterations in A549 cells such as shrinkage, detachment, membrane blabbing, and distorted shape when compared to control. The intact cell morphology in the control group was normal (Figure 5).

Lung cancer (A549) cells were treated with iron oxide nanoparticles (15 and 20 µg/mL) for 24 hours before being stained with the dual dye AO/EB and evaluated using fluorescence microscopy. Live cells have a typical nuclear appearance and glow green. Early apoptotic cells with ruptured nuclear membranes exhibit yellow fluorescence with condensed chromatin. Figure 6 shows a cell with chromatin condensation or fragmentation (uniformly red/orange-stained cell nuclei).

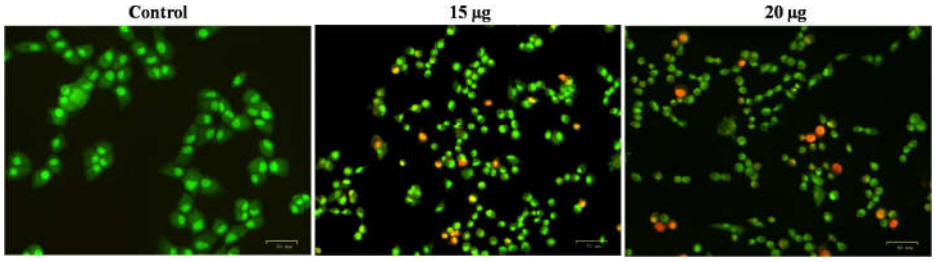

Figure 6. Apoptotic Staining – Control and sample 20 treated Lung Cancer A549 cells for 24 h.

Rhodamine 123 staining was used to determine the MMP of the cells. Rhodamine 123 is a cationic, cell-permeant green fluorescent dye used in membrane polarisation tests. The

fluorescence intensity directly reflects the cell's MMP. Control cells had brilliant green fluorescence, indicating that they were healthy. The MMP of cells lost on treatment, on the other hand, was dose-dependent. The complexes with a mass of 15 g showed the greatest MMP depletion (Figure 7).

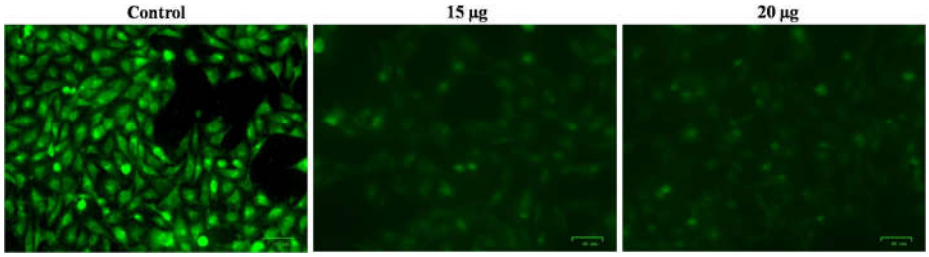

Figure 7. Mitochondrial membrane potential by Rhodamine 123 staining.

Rhodamine 123 is a fluorescent dye that can accumulate within the mitochondria due to its positive charge and lipophilic properties. It is sensitive to changes in mitochondrial membrane potential, and its fluorescence intensity is quenched at higher membrane potentials. Therefore, the level of Rhodamine 123 fluorescence can be used as an indicator of mitochondrial membrane potential.

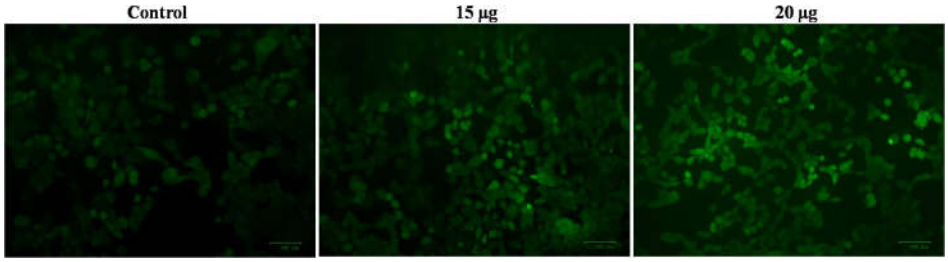

Figure 8. Detection of ROS using carboxy-H2DCFDA staining.

Several molecules in reactive oxygen species oxidise proteins and lipids (lipid peroxidation) and damage DNA and RNA (Figure 8). Reactive compounds containing oxygen include H_2O_2 (hydrogen peroxide), NO (nitric oxide), O_2 (oxide anion), peroxynitrite ($ONOO^-$), hypochlorous acid (HOCl), and hydroxyl radical (OH^-). Oxidative species are produced in pathogenic settings (cancers, ischemic/reperfusion, neurologic and cardiovascular pathologies, viral diseases, inflammatory diseases, autoimmune disorders, and so on), as well as physiological (non-pathological) circumstances such as cellular metabolism. Indeed, ROS play crucial roles in a range of cellular signalling pathways (such as proliferation, cell activation, and migration). Carboxy-H2DCFDA is not fluorescent, but it becomes fluorescent green when oxidised in the presence of ROS (Figure 8).

DNA fragmentation analysis is a common technique used to assess apoptotic cell death. In this study, DNA fragmentation was observed between control and treated lung cancer A549 cells after 24 hours. A positive control (iron oxide nanoparticles treated) could be DNA from cells treated with an apoptosis-inducing agent known to cause DNA fragmentation (Figure 9). The experiment observed significant morphological changes in A549 cells upon treatment with iron oxide nanoparticles. These changes included cell shrinkage, detachment, membrane blabbing, and

distorted shape, all of which are indicative of cellular stress and potential cell death. These alterations in cell morphology suggest that the iron oxide nanoparticles have a noticeable impact on the overall health and integrity of the cells [40]. The iron oxide nanoparticles could have significant implications for Targeted Lung Cancer A549 Cell Therapy by potentially improving drug delivery and crystallite size of iron nanoparticles used in Targeted Lung Cancer A549 Cell Therapy can significantly impact the therapy's effectiveness, drug loading, release kinetics, cellular uptake, biodistribution, toxicity, and imaging properties [41, 42].

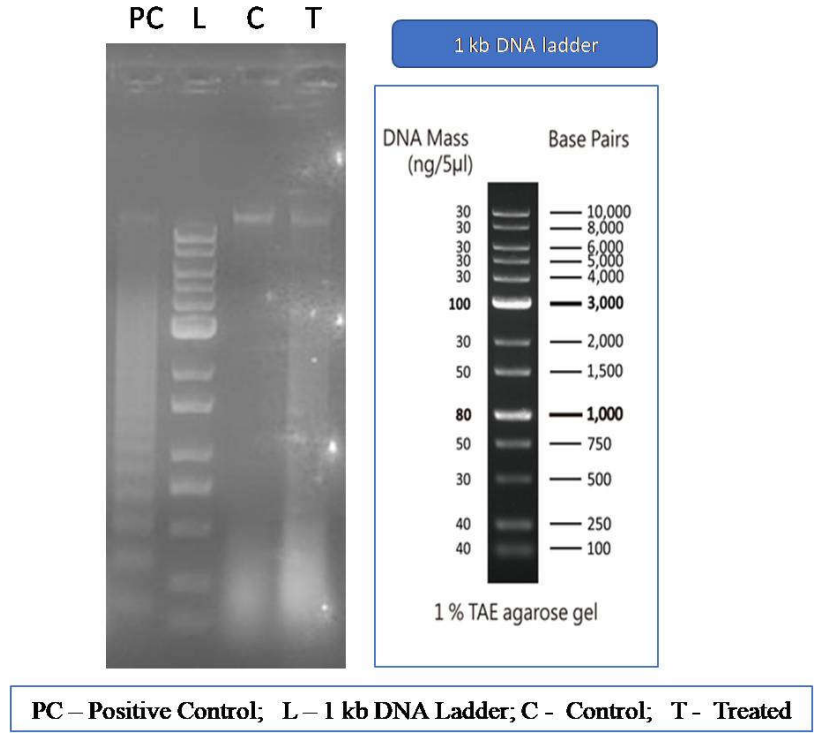

Figure 9. DNA fragmentation study – Control and Treated Lung Cancer A549 cells for 24 h.

The description indicates that the treated cells displayed characteristics of apoptosis. Some of these are broken nuclei, clumped chromatin, and different fluorescence patterns that can be seen with dual dye staining (AO/EB). The fact that there were early apoptotic cells with broken nuclei and late apoptotic cells with clumped or broken chromatin supports the idea that the iron oxide nanoparticles caused apoptosis in the A549 cells.

The study also looked at how iron oxide nanoparticles affect the health of mitochondria. This was done by using Rhodamine 123 to measure the potential of the mitochondrial membrane. The results showed a dose-dependent decrease in mitochondrial membrane potential, with greater depletion observed at the higher nanoparticle concentration (15 µg). This suggests that the nanoparticles could be influencing mitochondrial function and potentially contributing to the apoptotic processes observed.

The description discusses the generation of reactive oxygen species (ROS) in response to treatment. ROS are molecules that can damage cellular components, including DNA, RNA,

proteins, and lipids. The use of Carboxy-H2DCFDA dye allowed the detection of ROS production in treated cells [43]. The appearance of green fluorescence indicated the presence of ROS, suggesting that oxidative stress might be contributing to the observed cellular changes and apoptotic response.

The experiment also assessed DNA fragmentation, a hallmark of apoptotic cell death. The positive control involved iron oxide nanoparticles, which are known to induce apoptosis. This control helped confirm that the experiment was able to find DNA fragmentation and that the changes seen in the cells were linked to apoptotic processes.

CONCLUSION

Iron oxide nanoparticles were synthesized using *Spermacoce ocymoides* Burm.f. plant extracts as a reducing and stabilizing agent. The nanoparticles are characterized by FTIR, AFM, XRD and UV-Vis absorption spectroscopy analysis. The study highlights the impact of *Spermacoce ocymoides* plant extracts based on iron oxide nanoparticles on A549 lung cancer cells. The observed morphological changes, apoptotic characteristics, mitochondrial membrane potential depletion, ROS generation, and DNA fragmentation collectively suggest that the nanoparticles induce apoptosis and oxidative stress in the treated cells (A549 lung cancer cells). These findings contribute to a better understanding of the potential therapeutic effects of iron oxide nanoparticles in lung cancer treatment and emphasise the importance of studying their mechanisms of action on cellular processes.

ACKNOWLEDGMENT

This project was supported by Researchers Supporting Project number (RSP2023R177) King Saud University, Riyadh, Saudi Arabia.

REFERENCES

1. Thandra, K.C.; Barsouk, A.; Saginala, K.; Aluru, J.S.; Barsouk, A. Epidemiology of lung cancer. *Contemp. Oncol. (Pozn)*. **2021**, 25, 45-52.
2. Sung, H.; Ferlay, J.; Siegel, R.L.; Laversanne, M.; Soerjomataram, I.; Jemal, A.; Bray, F.; Global Cancer Statistics 2020: GLOBOCAN Estimates of Incidence and Mortality Worldwide for 36 Cancers in 185 Countries. *CA Cancer. J. Clin.* **2021**, 71, 209-249.
3. Dela Cruz, C.S.; Tanoue, L.T.; Matthay, R.A. Lung cancer: Epidemiology, etiology, and prevention. *Clin. Chest. Med.* **2011**, 32, 605-644.
4. Zappa, C.; Mousa, S.A. Non-small cell lung cancer: current treatment and future advances. *Transl. Lung. Cancer. Res.* **2016**, 5, 288-300.
5. Kim, A.S.; Ko, H.J.; Kwon, J.H.; Lee, J.M. Exposure to second hand smoke and risk of cancer in never smokers: A meta-analysis of epidemiologic studies. *Int. J. Environ. Res. Public Health* **2018**, 15, 1-17.
6. Kanwal, M.; Ding, X.J.; Cao, Y. Familial risk for lung cancer. *Oncol. Lett.* **2016**, 13, 535-542.
7. Xing, P.Y.; Zhu, Y.X.; Wang, L.; Hui, Z.G.; Liu, S.M.; Ren, J.S.; Zhang, Y.; Song, Y.; Liu, C.C.; Huang, Y.C.; Liao, X.Z.; Xing, X.J.; Wang, D.B.; Yang, L.; Du, L.B.; Liu, Y.Q.; Zhang, Y.Z.; Liu, Y.Y.; Wei, D.H.; Zhang, K.; Shi, J.F.; Qiao, Y.L.; Chen, W.Q.; Li, J.L.; Dai, M.; LuCCRES Group.; 2019 What are the clinical symptoms and physical signs for non-small cell lung cancer before diagnosis is made? A nation-wide multicenter 10-year retrospective study in China. *Cancer. Med*. **2019**, 8, 4055-4069.
8. Barta, J.A.; Powell, C.A.; Wisnivesky, J.P. Global epidemiology of lung cancer. *Ann. Glob. Health* **2019**, 85, 1-8.

9. Perez-Warnisher, M.T.; Carballosa de Miguel, M.P.; Seijo, L.M. Tobacco use worldwide: Legislative efforts to curb consumption. *Ann. Glob. Health.* **2018**, 84, 571-579.
10. Noronha, V.; Pinninti, R.; Patil, V.M.; Joshi, A.; Prabhash, K. Lung cancer in the Indian subcontinent. *South Asian J. Cancer.* **2016**, 5, 95-103.
11. Mishra, G.A.; Pimple, S.A.; Shastri, S.S. An overview of the tobacco problem in India. *Indian J. Med. Paediatr. Oncol.* **2012**, 33, 139-145.
12. Singh, A.; Ladusingh, L. Prevalence and determinants of tobacco use in India: Evidence from recent global adult tobacco survey data. *PLoS One* **2014**, 9, 1-12.
13. Furrukh, M. Tobacco smoking and lung cancer: Perception-changing facts. *Sultan. Qaboos. Univ. Med. J.* **2013**, 13, 345-358.
14. Walser, T.; Cui, X.; Yanagawa, J.; Lee, J.M.; Heinrich, E.; Lee, G.; Sharma, S.; Dubinett, SM. Smoking and lung cancer: The role of inflammation. *Proc. Am. Thorac. Soc.* **2008**, 5, 811-815.
15. Alberg, A.J.; Brock, M.V.; Ford, J.G.; Samet, J.M.; Spivack, S.D. Epidemiology of Lung Cancer: Diagnosis and Management of Lung Cancer, 3rd ed., American College of Chest Physicians Evidence-Based Clinical Practice Guidelines. *Chest.* **2013**, 143, e1S-e29S.
16. Yuan, M.; Huang, L.L.; Chen, J.H.; Wu, J.; Xu, Q. The emerging treatment landscape of targeted therapy in non-small-cell lung cancer - Signal transduction and targeted therapy. *Signal. Transduct. Target. Ther.* **2019**, 4, 1-14.
17. Cheng, Y.; Zhang, T.; Xu, Q. Therapeutic advances in non-small cell lung cancer: Focus on clinical development of targeted therapy and immunotherapy. *Medcomm.* **2021**, 2, 692-729.
18. Carrera, P.M.; Kantarjian, H.M.; Blinder, V.S. The financial burden and distress of patients with cancer: Understanding and stepping-up action on the financial toxicity of cancer treatment. *CA Cancer. J. Clin.* **2018**, 68, 153-165.
19. Choudhari, A.S.; Mandave, P.C.; Deshpande, M.; Ranjekar, P.; Prakash, O. Phytochemicals in cancer treatment: From preclinical studies to clinical practice. *Front. Pharmacol.* **2020**, 10, 1-17.
20. Tabish, S.A. Complementary and alternative healthcare: Is it evidence-based?. *Int. J. Health. Sci. (Qassim)* **2008**, 2, 5-9.
21. Ryang, J.; Yan, Y.; Song, Y.; Liu, F.; Ng, T.B.; Anti-HIV, antitumor and immunomodulatory activities of paclitaxel from fermentation broth using molecular imprinting technique. *AMB Express.* **2019**, 9, 1-10.
22. Thuy Pham, H.N.; Vuong, Q.V.; Bowyer, M.C.; Scarlett, C.J. Phytochemicals derived from *Catharanthus roseus* and their health benefits. *Technologies* **2020**, 8, 1-16.
23. Kuttan, R.; Bhanumathy, P.; Nirmala, K.; George, M. Potential anticancer activity of turmeric (*Curcuma longa*). *Cancer. Lett.* **1985**, 29, 197-202.
24. Esghaei, M.; Ghaffari, H.; Esboei, B.R.; Tapeh, Z.E.; Salim, F.B.; Motevalian, M. Evaluation of anticancer activity of *Camellia sinensis* in the Caco-2 colorectal cancer cell line. *Asian Pac. J. Cancer. Prev.* **2018**, 19, 1697-1701.
25. Park, G.H.; Park, J.H.; Song, H.M.; Eo, H.J.; Kim, M.K.; Lee, J.W.; Lee, M.H.; Cho, K.H.; Lee, J.R.; Cho, H.J.; Jeong, J.B. Anti-cancer activity of ginger (*Zingiber officinale*) leaf through the expression of activating transcription factor 3 in human colorectal cancer cells. *BMC Complement. Altern. Med.* **2014**, 14, 1-8.
26. Patino-Morales, C.C.; Jaime-Cruz, R.; Sanchez-Gomez, C.; Corona, J.C.; Hernandez-Cruz, E.Y.; Kalinova-Jelezova, I.; Pedraza-Chaverri, J.; Maldonado, P.D.; Silva-Islas, C.A.; Salazar-Garcia, M. Antitumor effects of natural compounds derived from *Allium sativum* on neuroblastoma: An overview. *Antioxidants* **2021**, 11, 1-11.
27. Szurpnicka, A.; Kowalczuk, A.; Szterk, A. Biological activity of mistletoe: in vitro and in vivo studies and mechanisms of action. *Arch. Pharm. Res.* **2020**, 43, 593-629.
28. Hong, H.; Baatar, D.; Hwang, S.G. Anticancer activities of ginsenosides, the main active components of ginseng. *Evid. Based. Complement. Alternat. Med.* **2021**, 8858006, 1-10.

29. Sanders, B.; Ray, A.M.; Goldberg, S.; Clark, T.; McDaniel, H.R.; Atlas, S.E.; Farooqi, A.; Konefal, J.; Lages, L.C.; Lopez, J.; Rasul, A.; Tiozzo, E.; Woolger, J.M.; Lewis, J.E. Anti-cancer effects of aloe-emodin: A systematic review. *J. Clin. Transl. Res.* **2017**, 3, 283-296.
30. Hosami, F.; Manayi, A.; Salimi, V.; Khodakhah, F.; Nourbakhsh, M.; Nakstad, B.; Tavakoli-Yaraki, M. The pro-apoptosis effects of *Echinacea purpurea* and *Cannabis sativa* extracts in human lung cancer cells through caspase-dependent pathway. *BMC. Complement. Med. Ther.* **2021**, 21, 1-12.
31. Savita, B.; Saritha, R.; Harshita, S.; Gangarapu, K. Synthesis, characterization and prediction of anticancer potentiality of some novel green nanoparticles by molecular docking and admet techniques. *Bull. Chem. Soc. Ethiop.* **2019**, 33, 493-504.
32. Yasmin, A.; Deribachew, B.; Ayalew, T.; Negussie, B.; Minbale, A.; Endale, T.; Meseret, A. Magnetic coffee residue biosorbent for selective extraction of zinc oxide nanoparticles in water samples. *Bull. Chem. Soc. Ethiop.* **2023**, 37, 859-873.
33. Priya; Naveen; Kamaljit, K.; Sidhu, A.K. Green synthesis: An eco-friendly route for the synthesis of iron oxide nanoparticles. *Front. Nanotechnol.* **2021**, 3, 1-16.
34. Yao, Y.; Zhou, Y.; Liu, L.; Xu, Y.; Chen, Q.; Wang, Y.; Wu, S.; Deng, Y.; Zhang, J.; Shao A. Nanoparticle-based drug delivery in cancer therapy and its role in overcoming drug resistance. *Front. Mol. Biosci.* **2020**, 7, 1-14.
35. Fakhar, U.D.; Aman, W.; Ullah, I.; Qureshi, O.S.; Mustapha, O.; Shafique, S.; Zeb, A. Effective use of nanocarriers as drug delivery systems for the treatment of selected tumors. *Int. J. Nanomedicine* **2017**, 5, 7291-7309.
36. Aida, M.S.; Alonizan, N.; Zarrad, B.; Hjiri, M. Green synthesis of iron oxide nanoparticles using Hibiscus plant extract. *J. Taibah Univ. Sci.* **2023**, 17, 1-9.
37. Riss, T.; Andrew Niles, M.S.; Rich Moravec, B.S.; Natashia Karassina, M.S.; Jolanta, V. Cytotoxicity Assays: In Vitro Methods to Measure Dead Cells. Assay Guidance Manual [Internet], Bethesda; **2019**; p 1.
38. Khan, I.; Morishita, S.; Higashinaka, R.; Tatsuma, D.M.; Yuji, A.; Erno, K.; Zoltan, H.; Sinko, K.; Luka, P.; Shiro, K. Synthesis, characterization and magnetic properties of -Fe_2O_3 nanoparticles prepared by sol-gel method. *J. Magnet. Magnet. Mater*. **2021**, 538, 1-11.
39. Das, R.; Witanachchi, C.; Nemati, Z.; Vijaysankar, K.; Irati, R.; Jose Angel Garcia Eneko, G.; Javier, A.; Vu, D.L.; Anh, T.L.; Manh, H.P.; Hariharan S. Magnetic vortex and hyperthermia suppression in multigrain ironoxide nanorings. *Appl. Sci*. **2020**, 10, 1-11.
40. Watanabe, M.; Yoneda, M.; Morohashi, A.; Hori, Y.; Okamoto, D.; Sato, A.; Kurioka, D.; Nittami, T.; Hirokawa, Y.; Shiraishi, T.; Kawai, K.; Kasai, H.; Totsuka, Y. Effects of Fe_3O_4 magnetic nanoparticles on A549 cells. *Int. J. Mol. Sci.* **2013**, 14, 15546-15560.
41. Alshammari, M.K.; Almomen, E.Y.; Alshahrani, K.F.; Altwalah, S.F.; Kamal, M.; Al-Twallah, M.F.; Alsanad, S.H.; Al-Batti, M.H.; Al-Rasheed, F.J.; Alsalamah, A.Y.; Alhazza, M.B.; Alasmari, F.A.; Abida Imran, M. Nano-enabled strategies for the treatment of lung cancer: Potential bottlenecks and future perspectives. *Biomedicines* **2023**, 11, 1-21.
42. Al Bostami, R.D.; Abuwatfa, W.H.; Husseini, G.A. Recent advances in nanoparticle-based Co-delivery systems for cancer therapy. *Nanomater.* **2022,** 12, 1-26.
43. Wu, D.; Yotnda, P. Production and detection of reactive oxygen species (ROS) in cancers. *J. Vis. Exp.* **2011**, 57, 1-4.